ACS SyntheticBiology

pubs.acs.org/synthbio

Research Article

Engineering Endosymbiotic Growth of *E. coli* in Mammalian Cells

Christoph G. Gäbelein, Michael A. Reiter, Chantal Ernst, Gabriel H. Giger, and Julia A. Vorholt*

Cite This: *ACS Synth. Biol.* 2022, 11, 3388–3396

Read Online

ACCESS | Metrics & More | Article Recommendations | Supporting Information

ABSTRACT: Endosymbioses are cellular mergers in which one cell lives within another cell and have led to major evolutionary transitions, most prominently to eukaryogenesis. Generation of synthetic endosymbioses aims to provide a defined starting point for studying fundamental processes in emerging endosymbiotic systems and enable the engineering of cells with novel properties. Here, we tested the potential of different bacteria for artificial endosymbiosis in mammalian cells. To this end, we adopted the fluidic force microscopy technology to inject diverse bacteria directly into the cytosol of HeLa cells and examined the endosymbiont-host interactions by real-time fluorescence microscopy. Among them, *Escherichia coli* grew exponentially within the cytoplasm, however, at a faster pace than its host cell. To slow down the intracellular growth of *E. coli*, we introduced auxotrophies in *E. coli* and demonstrated that the intracellular growth rate can be reduced by limiting the uptake of aromatic amino acids. In consequence, the survival of the endosymbiont-host pair was prolonged. The presented experimental framework enables studying endosymbiotic candidate systems at high temporal resolution and at the single cell level. Our work represents a starting point for engineering a stable, vertically inherited endosymbiosis.

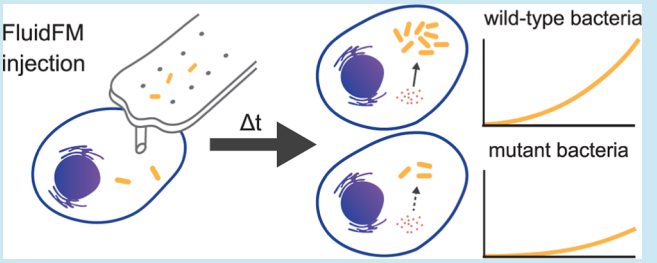

KEYWORDS: *endosymbioses, cytosolic bacteria, fluidic force microscopy, metabolic engineering, synthetic endosymbiosis*

INTRODUCTION

Endosymbioses are symbiotic relationships in which one partner, the endosymbiont, is incorporated within a living host cell. Endosymbiosis drives fundamental evolutionary developments by unifying two separate entities metabolically and genetically. The most prominent example for this process is eukaryogenesis: eukaryotic cells emerged from the intracellular symbiosis of an endosymbiotic bacterium related to Alphaproteobacteria and an archaeal host some 2 billion years ago.[1,2] More recent examples of endosymbioses exist, revealing common patterns in the evolution of host-endosymbiont pairs such as nutrient interdependencies and genome reduction of the endosymbiont.[3−6] These types of long-term biological interactions are widespread in nature. They are either based on vertical transmission of the endosymbiont to progeny or are facultative and horizontally acquired, as in legume plants where endosymbiotic bacteria fix nitrogen in exchange for nutrients and shelter.[7]

Synthetic endosymbioses have great potential for future biotechnological applications by directly linking two distinct chemical and metabolic compartments. Few groups have begun to explore the feasibility of such cell mergers. For example, by microinjection of algae or cyanobacteria into zebrafish eggs,[8,9] or by fusing *Escherichia coli* or *Mycoplasma mycoides*, with *Saccharomyces cerevisiae* cells.[10,11] Nevertheless, to date, a stable endosymbiont-host merger has not been demonstrated, and the required boundary conditions remain unexplored.

Two fundamentally different approaches can be used to introduce cells into cells to initiate artificial endosymbiosis: merging cells in bulk and microinjection. Merging cells in bulk utilizing polyethylene glycol-based protocols[10,12] has the advantage of mixing large numbers of cells and thus achieving potentially high throughput. However, due to low efficiencies at the single cell level, a selection regime for mergers is necessary, requiring an already stable endosymbiosis, including functional metabolic cooperation, coordinated cell division, and neglect adverse effects such as xenophagy or apoptosis. The initiation of a beneficial symbiosis thus remains a major challenge. To reduce the complexity of the task, direct injection of bacteria into host cells and subsequent microscopic analysis represents an alternative to engineering endosymbiotic systems at the single cell level. This allows the observation of newly created host-endosymbiont pairings in real time. Delivery of bacteria into the cytosol of mammalian cells has been shown using microinjection.[13,14] Among enabling technologies, fluidic force microscopy (FluidFM) is particularly promising. The technology features atomic force microscopy (AFM) that connects the ability of microinjection

Received: June 2, 2022
Published: October 4, 2022

https://doi.org/10.1021/acssynbio.2c00292
ACS Synth. Biol. 2022, 11, 3388–3396

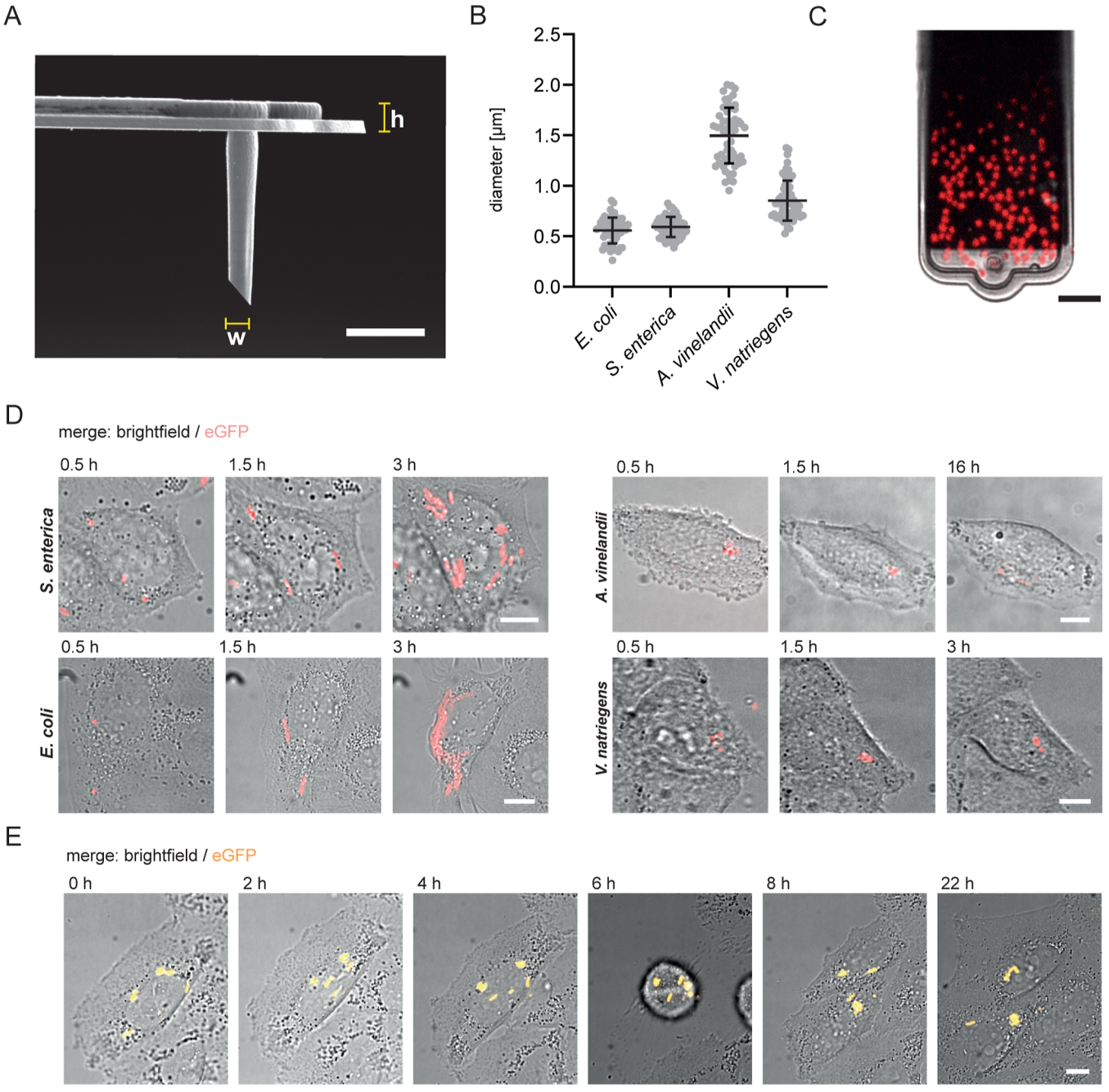

Figure 1. Injection of bacteria into mammalian cells using FluidFM. (A) Focused ion beam image of a FluidFM cantilever with a cylindrical apex, h describes the height of the microfluidic channel inside the probe, and w the width of the cylindrical apex used for cell insertion. Scale bar = 5 μm. (B) Measurement of cell diameters of selected bacterial strains. Horizontal bars indicate mean value, vertical bars indicate standard deviation of each strain: *E. coli*: 0.56 ± 0.13 μm, *S. enterica*: 0.59 ± 0.10 μm, *A. vinelandii*: 1.50 ± 0.27 μm, and *V. natriegens*: 0.85 ± 0.20 μm. (C) Fluorescent microscopy overlay of the FluidFM cantilever (brightfield, gray) loaded with fluorescently labeled *A. vinelandii* cells (fluorescent, red). Scale bar = 10 μm. (D) Fluorescent microscopy overlay images of HeLa cells (gray) post bacterial (red) injection over time. For used fluorescent labels see Material and Methods section and Table S2. Scale bars = 10 μm. (E) Fluorescent time-lapse microscopy images of non-proliferating, fluorescently labeled *E. coli* cells (eGFP, yellow) inside HeLa cells over one cell division. Scale bar = 10 μm.

devices to dispense small volumes (fL—pL) with high spatial precision while preserving cell viability.[15−17] Here, we have expanded the toolbox of the FluidFM platform to introduce à priori non-pathogenic bacterial strains (*Azotobacter vinelandii*, *Vibrio natriegens*, and *E. coli*) as well as a pathogenic bacterium (*Salmonella enterica*), into HeLa cells, to analyze their growth behavior in the cytosol. We explore the impact of rationally designed metabolic *E. coli* mutants with the long-term goal to match their growth to that of cultured mammalian cells as the designated host organism. Our approach allows exploration of genetic and physiological impacts of reduced metabolic capabilities of the symbiont and their impact on the stability of the host-endosymbiont relationship.

RESULTS

Injection of Bacteria into HeLa Cells. For this study, we selected three different gammaproteobacteria that could be promising candidates for artificial endosymbioses due to their

https://doi.org/10.1021/acssynbio.2c00292
ACS Synth. Biol. 2022, 11, 3388−3396

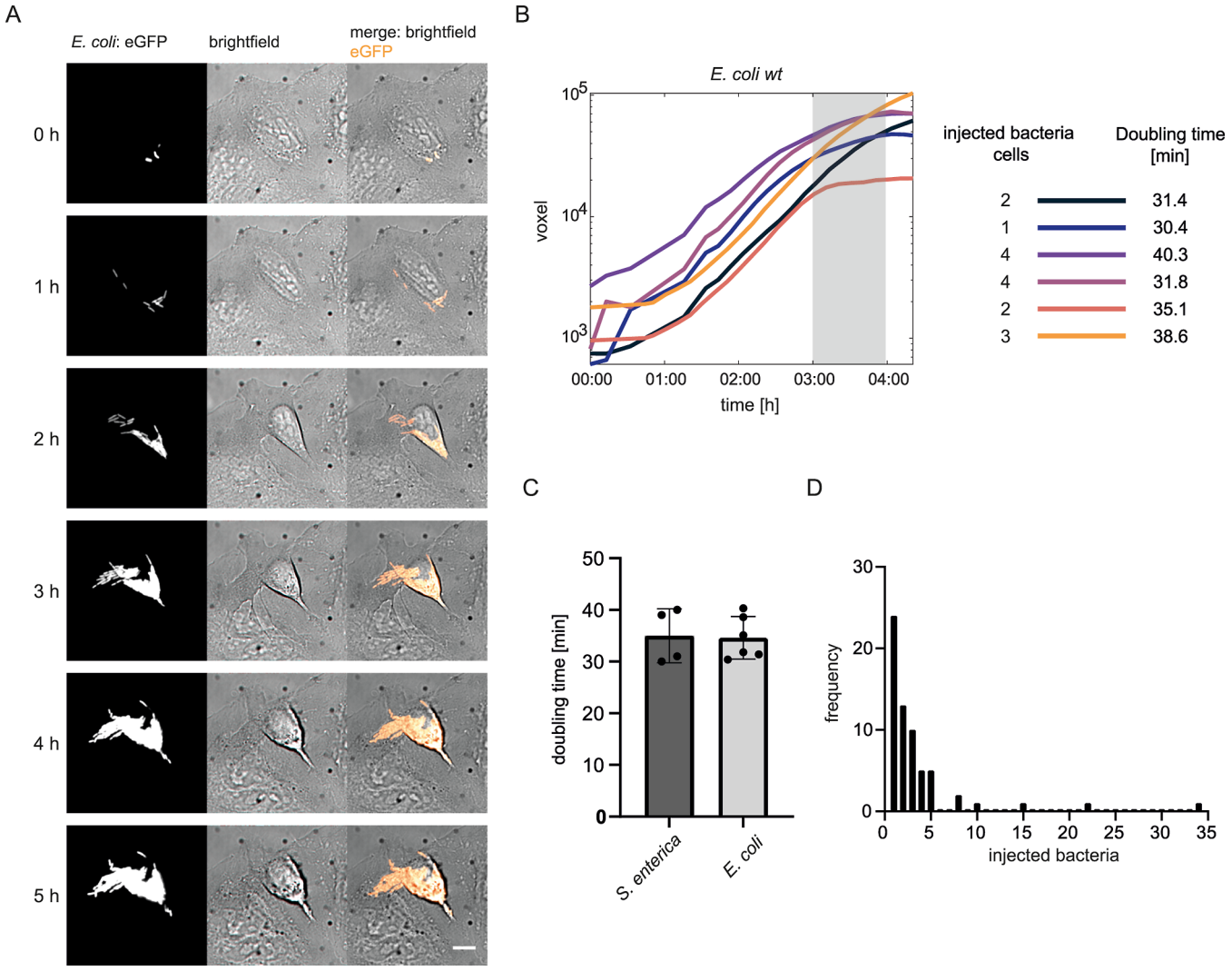

Figure 2. Doubling times of *E. coli* cells in the cytoplasm of HeLa cells. (A) Fluorescent time-lapse microscopy images of proliferating, fluorescently labeled *E. coli* cells (eGFP, yellow) inside HeLa cells over time. Scale bar = 10 μm. (B) Counting of *E. coli* fluorescent voxels over time in HeLa cells, each curve shows growth of *E. coli* in an individual HeLa cell. Gray area marks timeframe when intracellular growth ceased. Number of initially injected bacteria and corresponding doubling times are depicted on the right. (C) Calculated intracellular doubling times of *E. coli* (35 ± 4 min) and *S. enterica* (35 ± 5 min). (D) Frequency distribution of injections into single HeLa cells.

biosynthetic capabilities and genetic tractability: *E. coli* (K-12) *V. natriegens*, and *A. vinelandii*. Furthermore, these strains cannot naturally invade host cells, preventing cross-infections in cell cultures[18] that would compromise long-term experiments in the future. As a premise, the candidates need to be able to proliferate in the cytosol of mammalian cells, which has generally been described not to be permissive for bacterial growth.[13] Therefore we included the pathogenic strain *S. enterica* as a positive control because the bacterium is known for its ability to grow in the cytosol of mammalian cells.[18] To enable fluidic handling and injection of the bacteria, we used cylindrical FluidFM probes.[19] To freely move within the microfluidic channel of the cantilevers, the minimal Feret diameter of the bacteria needs to be smaller than the channel dimensions of the probe (Figure 1A). We therefore measured the diameters of the chosen bacteria (Figure 1B) and found that *E. coli*, *V. natriegens*, and *S. enterica* can be handled with a channel width of 1.2 μm, while *A. vinelandii* requires a larger channel width of 1.6 μm (Figure 1C). More detailed information on the bacterial injection protocol is available in the Materials and Methods section.

In a first set of experiments, we injected fluorescently labeled *S. enterica* bacteria into the cytosol of cultured HeLa cells. Because *S. enterica* is generally able to grow in the cell culture media (Table S1), we ensured that the observed growth is purely intracellular by adding gentamicin to the culture media. Gentamicin is a bactericidal antibiotic that does not pass eukaryotic membranes, hence cytoplasmic bacteria are protected.[20] As expected, we observed the robust cytosolic growth of *S. enterica*, as evidenced by the proliferation of the GFP-tagged bacteria 3 h post injection (Figure 1D). Next, we injected the fluorescently labeled bacteria that are not known to proliferate in the cytosol. In three experimental replicates, *V. natrigens* and *A. vinelandii* were unable to replicate intracellularly. While *A. vinelandii* was apparently unable to proliferate in the cytosolic compartment, *V. natriegens* cells disintegrated within the first 2 h post injection, staining the cytosol of HeLa cells with GFP (see Movie S1). The commensal *E. coli* showed robust intracellular growth, which

https://doi.org/10.1021/acssynbio.2c00292
ACS Synth. Biol. 2022, 11, 3388−3396

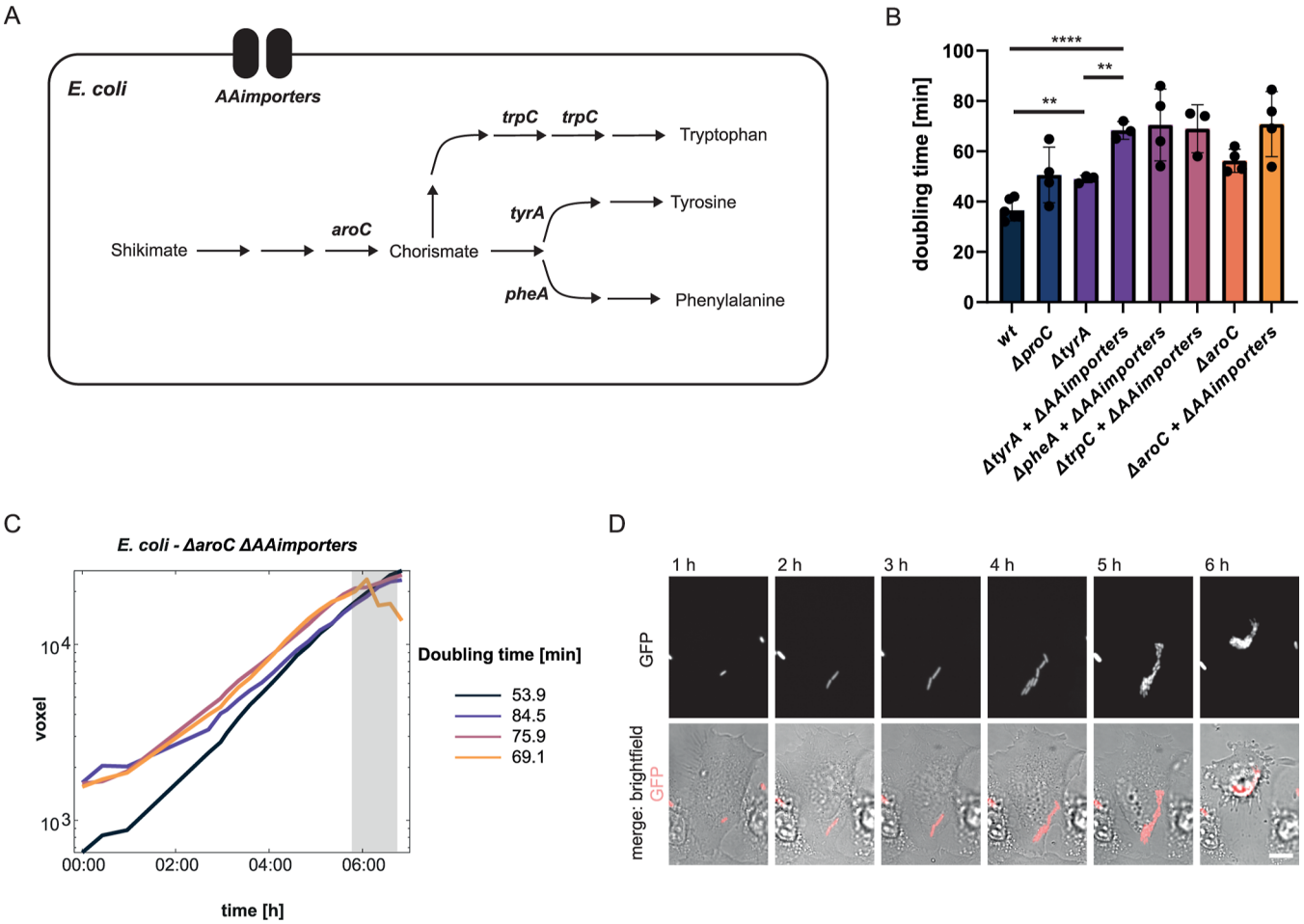

Figure 3. Intracellular growth of *E. coli* metabolic mutants. (A) Schematic metabolic pathway map for the synthesis of aromatic amino acids of *E. coli* and aromatic amino acid importers. (B) Intracellular doubling times of *E. coli* wt and tested metabolic mutants: wt: 35 ± 4 min, Δ*proC*: 50 ± 10 min, Δ*tyrA*: 49 ± 1 min, Δ*tyrA*, Δ*AAimporters* (Δ*tyrP*, Δ*tnaB*, Δ*aroP*, Δ*pheP*, Δ*mtr*, Δ*hisPMQJ*, Δ*proY*, *livHMGKF*::Cam): 68 ± 3 min, Δ*pheA*, Δ*AAimporters*: 71 ± 12 min, Δ*trpC*, Δ*AAimporters*: 69 ± 8 min, Δ*aroC*: 56 ± 4 min, Δ*aroC*, Δ*AAimporters*: 70.9 ± 11 min. (C) Counting of *E. coli* Δ*aroC*, Δ*AAimporters* fluorescent voxels over time in HeLa cells, each curve shows bacterial growth in an individual HeLa cell. Gray area marks timeframe when intracellular growth ceased. (D) Fluorescent time-lapse microscopy images of proliferating, fluorescently labeled *E. coli* Δ*aroC*, Δ*AAimporters* cells (eGFP, yellow) inside HeLa cells over time. Scale bar = 10 μm.

contrasts with earlier observations where only an enteroinvasive *E. coli* strain was able to replicate in the cytosolic compartment.[13]

HeLa cells harboring proliferating *S. enterica* or *E. coli* cells perished within a few hours post injection. This observation correlated with the decrease in integrity of the cytoplasmic membrane, which we tracked by the influx of the dye DRAQ7, which stains only permeabilized mammalian cells.[21] Visible dye influx can only be detected after considerable bacterial growth (Figure S1). Still, the question remained open whether loss of viability occurs non-specifically due to an increasing metabolic burden caused by the bacteria, or due to an apoptotic program induced by bacterial presence.[22] Therefore, we tested whether HeLa cells are still able to proliferate when injected with non-proliferating *E. coli* cells by injecting the bacteria in the presence of the bacteriostatic antibiotic chloramphenicol. We followed 30 injected HeLa cells in a time-course experiment for over 20 h. In all of them, the bacteria remained visible without multiplying (Figure 1E). When the host cell divided, the bacterial cells were partitioned seemingly at random between both daughter cells (Figure 1E). This pattern remained constant throughout the series of experiments in this study: whenever *E. coli* cells failed to replicate intracellularly, the viability of the host cell was unaffected, and it continued to proliferate while containing bacterial cells.

We conclude that injection of bacteria directly into the cytosol of HeLa cells with FluidFM works reliably and does not affect host cell viability upon injection. It is thus a powerful approach to investigate intracellular growth of different bacterial species, including commensal *E. coli* strains.

Evaluation of Doubling Times of Intracellularly Growing *E. coli* Wild Type Cells. The observations described above revealed that *E. coli* can proliferate until it occupies a large portion of the cytoplasmic volume, and that HeLa cells generally tolerate the presence of *E. coli* cells in their cytoplasm but eventually disintegrate, coinciding with excessive intracellular proliferation of the bacterium. Host cells showed early signs of stress (1−2 h post injection, ∼20 intracellular *E. coli* cells) manifesting itself in detachment from the substrate before finally lysing after 3−4 h post injection. To analyze the doubling time of *E. coli* cells in the cytoplasm of single HeLa cells, we developed an approach to quantify *E. coli* cell volume from Z-stack images, by counting the total amount of fluorescent voxels from fluorescent bacteria over time

https://doi.org/10.1021/acssynbio.2c00292
ACS Synth. Biol. 2022, 11, 3388−3396

(Figures 2A,B and S2). The intracellular doubling time of *E. coli* of T_d = 35 ± 4 min (Figure 2C) was higher than on LB media (T_d = 22 ± 2 min, Table S1), but lower than in cell culture media (T_d = 57 ± 8 min, Table S1). Notably, intracellular bacteria showed a short lag-phase, followed by exponential growth and a stationary phase. The end of the exponential growth phase coincided with influx of DRAQ7, marking permeability of the cytoplasmic membrane of HeLa cells. Presence of an exponential growth phase suggests that the bacteria in the cytoplasm do not experience initial growth limitation due to nutrient pool depletion. The FluidFM approach allowed the injection of single and multiple *E. coli* cells into the cytoplasm of individual HeLa cells, enabling starting points of single or multiple endosymbionts per host (Figure 2D). We tested whether the doubling time was influenced by the number of bacteria initially injected (here: 1−4 bacterial cells). No effect on bacterial growth speed was observed (Figure 2B), consistent with the exponential growth, until more than 20 bacterial cells were present in the host cells. The calculated doubling time is comparable to the intracellular doubling time previously observed for *Shigella flexneri* cells (T_d = 37 ± 4 min),[23] a pathogenic relative of the commensal *E. coli* harboring similar metabolic capabilities. Growth analysis of injected *S. enterica* cells resulted in a similar doubling time of 35 ± 5 min (Figure 2C), which again was higher compared to LB (T_d = 24 ± 1 min) and lower compared to the cell culture media (T_d = 41 ± 2 min).

Intracellular Growth Speed of *E. coli* Metabolic Mutants in Single Cells. The intracellular growth of *E. coli* led to collapse of the fused systems approximately 3 h after its initiation (see gray area Figures 2B and S1 and S3). Evidently, the growth of the bacteria must be slowed down to achieve a stable merger between *E. coli* and HeLa cells. Metabolomic studies suggest that the pool of metabolites in HeLa cells is dominated by free amino acids (~80% of metabolites in central carbon metabolism),[24] constituting a rich source of carbon and energy for the cytosolic growth of *E. coli*. To ensure that *E. coli* was dependent on this pool, we used an auxotrophic mutant deficient in tyrosine biosynthesis Δ*tyrA* (Figure 3A). The mutant grew slightly slower intracellularly than the wild-type (T_d = 49 ± 7 min) (Figure 3B). To now limit amino acid import from the cytosol, we then tested a nonuple mutant, in which in addition to *tyrA*, also the aromatic and branched chain amino acid importers Δ*tyrP*,[25] Δ*tnaB*,[26] Δ*aroP*,[27] Δ*pheP*,[28] Δ*mtr*,[29] Δ*hisPMQJ*,[30] Δ*proY*,[31] *and livHMGKF*::*Cam*[32,33] (Δ*tyrA*, Δ*AAimporters*) were mutated. The strain was unable to grow in M9 minimal media supplemented with tyrosine (Table S1). Intracellularly, the strain grew at a doubling time of 68 ± 3 min. In addition, we tested single mutations of *trpC* and *pheA* that are required for the biosynthesis of the amino acids tryptophan and phenylalanine, respectively, in the genetic background of the Δ*AAimporters* strain. These nonuple mutants yielded similar doubling times of 69 ± 8 min (Δ*trpC*, Δ*AAimporters*) and 68 ± 3 min (Δ*pheA*, Δ*AAimporters*). Simultaneous abolishment of the synthesis of all three aromatic amino acids can be achieved by knocking out the *aroC* gene (Figure 3A). Again, the knockout of *aroC* alone reduced the doubling time to 56 ± 8 min, while the mutations of the Δ*AAimporters*—strain introduced an additive effect, increased the doubling time to 70 ± 11 min (Figure 3B−D).

The slower growth rate of *E. coli* resulting from the introduction of amino acid auxotrophies had a direct impact on the longevity of the cellular merger. It effectively extended the time of intracellular growth of *E. coli* and HeLa from slightly over 3 h up to 6 h (Figure 3C,D), affirming the potential to alter metabolism toward sustainable intracellular growth.

DISCUSSION

In this study, we introduce FluidFM as an efficient tool to inject bacteria into cultured cells while preserving viability of both organisms. Recently developed FluidFM cantilevers with cylindrical apexes[19] allow injection of diverse bacteria. We deduced intracellular growth from individual injected host cells using diverse fluorescently labeled bacteria.

While intracellular growth of enteroinvasive *E. coli* strains has been well documented,[34] injection of commensal *E. coli* strains has yielded inconsistent results in previous studies.[13] In our experiments using the minimally invasive FluidFM approach, the commensal laboratory K-12 strain BW25113 showed robust intracellular growth. We also tested other gammaproteobacteria and found that these were unable to replicate inside the cytosol of HeLa cells. Whether the cytosol is generally growth permissive for bacteria in terms of nutrient availability, osmolarity and pH, is under debate. These parameters may vary between cell types and organisms and are speculated to dictate niches of invasive bacteria.[35,36] The observation that *V. natriegens* lysed rapidly inside the cytosol may hint toward osmotic stress experienced by the halophilic bacterium. Recently, we have shown that FluidFM can also be used to inject liquids into hard-wall cells including fungal cells,[37] opening up the opportunity to test injection of larger objects, including bacteria, into a wider variety of eukaryotic organisms. This could then allow to address the question which metabolic pre-adaptations are required for bacteria to grow in a given host range.

Furthermore, we demonstrate that the use of fluorescence microscopy for the evaluation of total bacterial cell volume provides a powerful means by which the intracellular growth behavior of bacteria can be quantified. In our system, the merger collapses after a few hours. However, we show that the intracellular growth rate can be slowed by introducing auxotrophies in amino acid synthesis and uptake (shown here for aromatic amino acids, Figure 3). Although the auxotrophs were unable to grow in minimal medium without supplementation of the respective amino acid (Table S1), growth of *E. coli* was rescued intracellularly. The underlying reason for the auxotrophy rescue is currently unclear, but we speculate that the uptake of short peptides might be a promising target to investigate in the future. Preliminary tests revealed that the Δ*aroC* strain in M9 minimal media supplemented with Casein hydrolysate, providing a source of short peptides, showed a doubling time of larger than 200 min (Table S1). It will be of interest to test whether oligopeptide importer knockouts slow down intracellular growth even more. Throughout the project, we tested additional strategies to tune *E. coli* growth (Figure S4). Mutations in purine metabolism led to defects in cell division during intracellular growth of *E. coli*, a similar effect was induced by the addition of carbenicillin to the media resulting in elongated *E. coli* cells extending over 10 μm (Figure S4). A defect in synthesis of the cofactor biotin showed no effect in *E. coli* growth (Figure S4). Additionally, we tested an *E. coli* HS strain deficient in the biosynthesis of D-alanine,[38] a component of the peptidoglycan layer. The strain was able to divide once intracellularly, while losing its rod shape and disintegrating (Figure S4). We conclude that the

https://doi.org/10.1021/acssynbio.2c00292
ACS Synth. Biol. 2022, 11, 3388−3396

cytoplasm is generally growth permissive for *E. coli* cells; however, restricting the intracellular growth may induce pleiotropic effects preventing sustained growth. Our data suggest that the strategy to limit growth via amino acid uptake in conjunction with amino acid auxotrophy is promising to be explored further, as a high metabolic flux is required to sustain growth enabling quick feedback on growth speed. In addition, a mutualistic symbiosis in which *E. coli* strains provide nutrients for HeLa cells would then allow selection for functional symbioses. Ideally, this would be an essential metabolite that can be provided by few endosymbiotic cells.

Endosymbionts in nature undergo massive reduction of genome size, simultaneously shrinking their network of metabolic pathways as observed, for example, in the genus of *Buchnera*.[39] "Slimmer" genomes, also observed in obligate pathogenic bacteria, are speculated to be the result of Muller's Ratchet.[39,40] We argue that gene loss also has a stabilizing effect on the host-endosymbiont relationship by enhancing interdependencies and paralleling growth rates. Constriction of the endosymbiont genome could also purge non-beneficial metabolic interactions, leading to a systemic gain of fitness.[41]

Our real-time observations of growth arrested *E. coli* cells suggest that random repartitioning of cells during mitosis can occur (Figure 1E). Assuming random transfer of endosymbionts to daughter cells, the merger does not necessarily require perfectly synchronized growth rates because some progenitor cells will receive low amounts of endosymbionts, enabling further proliferation, while others will drop out containing excessive amounts of endosymbionts. Therefore, host endosymbiont pairs might be relatively tolerant toward doubling time mismatches, as long as the host cell is still able to divide.

In summary, we present a strategy toward engineering host-endosymbiont systems that will provide new insights into host-endosymbiont evolution and new opportunities in biotechnology and synthetic biology.

MATERIAL AND METHODS

Bacterial Cultures. For a list of all strains and plasmids see Table S2.

E. coli and *S. enterica* cells were grown at 37 °C in Luria-Bertani (LB, Sigma-Aldrich, USA) agar plates, supplemented, when needed, with kanamycin (50 μg/mL, Roth) or streptomycin (50 μg/mL, AppliChem). *E. coli* strains were fluorescently labeled with plasmid pGFP, *S. enterica* strains were fluorescently labeled with plasmid pM965. *A. Vinelandii* cells were grown on standard B media[42] at 28 °C, the cells were tagged with GFP using the bjGFP plasmid, media were supplemented with tetracycline (10 μg/mL, Sigma-Aldrich, USA) if needed. *V. natriegens* was grown on a LB3 medium (LB + NaCl fc. 3% w/v) at 37 °C and fluorescently labeled using a sfGFP plasmid, and the expression was induced over night with anhydrotetracycline (500 ng/mL, Adipogen. USA). For experiments, all strains were grown to stationary phase via incubation for 48 h, except *E. coli* strain Δ*aroC* Δ*AAimporters*, which was incubated for 20 h at 28 °C.

Cell Culture. HeLa cells were maintained in Dulbecco's Modified Eagle Medium containing 1% penicillin−streptomycin (ThermoFisher, USA) and 10% fetal bovine serum (ThermoFisher, USA) culture medium at 37 °C and in a humidified incubator at 5% CO_2 concentration (Memmert, Germany). Cells were seeded 24 to 48 h preceding an experiment onto 50 mm tissue-culture-treated low μ-dishes (ibidi, Germany) inside two-well culture inserts (ibidi, Germany). For the injection experiments, cells were washed and subsequently cultured using a CO_2-independent growth medium containing 10% FBS (ThermoFisher, USA). When required, DRAQ7 was added to the culture media preceding the bacterial injection procedure (see below) following manufacturer's instructions (Life Technologies, USA).

FluidFM Setup and Microscopy. The FluidFM setup consists of a FlexAFM 5-NIR scan head controlled by a C3000 controller (Nanosurf, Switzerland), a pressure controller (ranging from −800 to +1000 mbar, Cytosurge), and microfluidic atomic force microscopy probes (Cytosurge, Switzerland and SmartTip, The Netherlands). The scan head is mounted on an inverted AxioObserver microscope equipped with a temperature-controlled incubation chamber (Zeiss, Germany). The microscope is coupled to a spinning disc confocal microscope (Visitron, Germany) with a Yokogawa CSU-W1 scan head and an EMCCD camera system (Andor, UK). For the creation of images and videos, a 63× oil objective with 1.4 numerical aperture was used, 4.85 pixel/micron; images were acquired in 16 bit format. Image acquisition was controlled using the VisiView software (Visitron, Germany); linear adjustments and video editing were made with Fiji.[43] Images and movies showing fluorescently labeled bacteria (Figures 1, 2, 3, and S1 and Movies S1 and S2) were created by summing up fluorescence from Z-stacks and subsequently reconverted into 16 bit format using Fiji. The paper uses the "thermal" colormap originating from Thyng et al.[44]

FluidFM Probe Processing and FIB-SEM Imaging and Milling. Cylindrical FluidFM-probes were prepared as in Gäbelein et al.[19] The used protocol only deviates in the used FIB-scanning electron microscopy (SEM) imaging setup: for the current paper, a Helios 5UX DualBeam FIB-SEM setup (ThermoFisher, USA) was used. The image in Figure 1A was taken using FIB-imaging.

Generation of *E. coli* Deletion Strains. Plasmid and genomic locus maps are provided in Supporting Information file 1.

Individual genes were deleted from the *E. coli* genome using CRISPR-Cas9-assisted recombineering as described by Jiang and co-workers.[45] For a given locus, we chose the best validated guide RNA corresponding to Guo et al.,[46] and cloned it into a modified pTargetF plasmid using Gibson assembly (New England Biolabs, USA). The plasmid, pTargetF_sacB, carried the *Bacillus subtilis sacB* gene which confers susceptibility to sucrose and enables counterselection against the plasmid. The exact deletion was encoded by the ssDNA oligo.[47] The editing protocol was as follows: an *E. coli* carrying pCas plasmid was inoculated in a 2 mL SOB medium supplemented with kanamycin in a culture tube and grown overnight at 30 °C, 220 rpm. This culture was diluted 50-fold into a 3 mL fresh SOB medium (0.5% (w/V) yeast extract, 2% (w/V) tryptone, 10 mM sodium chloride, 2.5 mM potassium chloride, and 20 mM magnesium sulfate. SOC medium is SOB medium supplemented with 20 mM glucose. If indicated, antibiotics were added in the following concentrations (mg L^{-1}): 50 kanamycin, 20 streptomycin sulfate) supplemented with kanamycin and grown to mid-exponential phase (OD_{600} 0.4−0.7). At this point, expression of recombineering enzymes was induced with 10 mM L-arabinose, and the culture was incubated for 27 min. 2 mL of the culture was harvested by centrifugation (4 °C, 5000*g*, 2 min) and made electrocompetent by washing five times with 1 mL of ice cold 10%

https://doi.org/10.1021/acssynbio.2c00292
ACS Synth. Biol. 2022, 11, 3388−3396

(V/V) glycerol. 100 ng of pTargetF_sacB plasmid and ssDNA oligo to a final concentration of 5 μM were added to the electrocompetent cells and electroporated using a Bio-Rad MicroPulser Electroporator (Bio-Rad, Switzerland). Subsequently, cells were recovered in a 1 mL SOC medium for 2 h and streaked out on an agar plate containing LB medium supplemented with kanamycin and streptomycin which was incubated overnight at 30 °C. Successful deletion of a locus was confirmed by colony PCR. pTargetF_sacB plasmid was cured by streaking out strains on agar plates containing LB medium supplemented with 10% (w/V) sucrose and kanamycin and incubated overnight at 30 °C.

Bacteria Injection Using FluidFM. Before each experiment, the cantilevers were cleaned by a 60 s plasma treatment (Plasma Cleaner PDG-32G, Harrick Plasma) before coating overnight with vapor phase SL2 Sigmacote (Sigma-Aldrich, USA) in a vacuum desiccator. The siliconized probe was subsequently oven-dried at 100 °C for 1 h. The cantilever spring constant was measured using software-implemented scripts (cylindrical probes: 1.5 ± 1 Nm^{-1}). Bacterial cultures were scraped off agar plates, washed three times in HEPES-2 buffer (10 mM HEPES, 150 mM NaCl, pH = 7.4), and adjusted to an optical density at 600 nm (OD_{600}) of 1.5, then 15 μL of the bacterial culture were filled into the microfluidic system of the used FluidFM probe. Subsequently, the probe was moved to a region containing cells targeted for injection. For injection of bacteria, the probe was positioned above a target cell in proximity, but never directly over, the nucleus. The cantilever was then inserted into the cell using a force setpoint of 100 nN, and subsequently retracted for 300 nm before the bacteria were injected by applying 40 mbar positive pressure. The injection process is controlled by observing the process in brightfield in real-time where the positive pressure is held until the cell visibly inflates, allowing injection of ∼100 fL to 1 pL while maintaining cell viability.[17] Subsequently the pressure of the microfluidic system is set to 0 mbar and the probe is retracted and moved to the next cell. Injection of a single cell, including the targeting and retraction process, takes less than 2 min. Therefore, the approach enables injection of >100 cells per day and is mostly limited by the capability of the microscope setup to follow bacterial growth in the injected cells at sufficient resolution. The workflow presented in this work was optimized for cultured cells under a 63× oil objective (see "FluidFM setup and microscopy" above). Host cell viability post injection depends on the injected volume, which can be tuned by setting the positive pressure value of the fluidic system and the time of injection, as previously characterized for this probe type[19] and other FluidFM probes.[17] Following injection, bacteria only start to proliferate in a subset of injected cells, these cells were subsequently used to quantify the doubling time. As soon as the desired number of cells was injected, gentamicin (Axon Lab, Switzerland) was added into the culture media to a final concentration of 20 μg/mL, the AFM scan head was removed from the microscopy setup and the ibidi μ-dish, 50 mm low (ibidi, Germany), was sealed from evaporation using the provided lid. Movie S2 shows a full recorded frame of HeLa cells injected wild-type *E. coli* cells.

Evaluation of Bacterial Voxel Number from Z-Stack Images. The MatlabR2020b code is available at https://gitlab.ethz.ch/cgaebele/engineering-endosymbiotic-growth-of-e-coli/

In short: for an individual timepoint, a Z-stack image of *E. coli* inside of viable HeLa cells was taken imaging the full range in Z in which fluorescent signal could be detected using a step size of 500 nm. Subsequently, the images were loaded into MatlabR2020b (MathWorks, USA). For these Z-stack images, the fluorescent background remained steady at ∼500 (16 bit images); hence, pixels having a fluorescence value of 1000 (2× background level) were then counted as voxels belonging to a fluorescent *E. coli* cell. Furthermore, only voxels within a manually outlined region of interest were counted. The program also evaluates the average fluorescence levels of the imaged *E. coli* cells because the bacteria may shift in their fluorescence levels during the measurement leading to false results. Growth curves were obtained using timeframes in which the voxel number increases linearly when plotted on a logarithmic axis and in which the average fluorescence level remained stable.

Measurements of Bacterial Growth Rates in Media. The bacterial strains were grown on plate as done in preparation for bacteria injection experiments, see above. Subsequently, the strains were transferred to the tested media condition at an adjusted OD_{600} of 0.05 inside a single well in a 96-well plate (flat bottom, TPP). Each growth condition was tested in triplicates. Tested media: LB (Sigma-Aldrich, USA), CO_2-free media (ThermoFisher, USA), and M9 minimal medium with (g* L^{-1}): 20 glucose, 6.78 Na_2HPO_4, 3 KH_2PO_4, 0.5 NaCl, 1 NH_4Cl, 0.049 $MgSO_4{\cdot}7H_2O$, 0.0015 $CaCl_2{\cdot}2H_2O$, 0.34 thiamine hydrochloride, trace elements (mg*L^{-1}) 0.5 $FeCl_3{\cdot}6H_2O$, 0.09 ZnSO4·$7H_2O$, 0.088 $CuSO_4{\cdot}5H_2O$, 0.045 $MnCl_2$, 0.09 CoCl2·$6H_2O$, if indicated M9 media was supplemented with 100 μM tyrosine (Y), tryptophan (W), phenylalanine (F), or 1% w/v casein hydrolysate. Growth curves were measured at a wavelength 600 nm for 24 h in a LogPhase 600 plate reader (Biotek, USA) at 37 °C and subsequently evaluated in Excel (Microsoft, USA).

Statistics and Reproducibility. All shown experiments were repeated at least three times independently. Shown microscopy images were chosen as representative images. Performed statistical testes and significance levels were indicated in the text, figure legends, or supplementary files.

■ ASSOCIATED CONTENT

Supporting Information

The Supporting Information is available free of charge at https://pubs.acs.org/doi/10.1021/acssynbio.2c00292.

HeLa cell injected with *V. natriegens* cells and immediately traced using time-lapse fluorescence microscopy (AVI)

Overlay timelapse of brightfield, green, and red fluorescent channels (AVI)

DRAQ7 influx into HeLa cells, quantification of *E. coli* cell growth, additional *E. coli* mutants tested for intracellular growth, and additional information on the tested *E. coli* strains in this study (PDF)

■ AUTHOR INFORMATION

Corresponding Author

Julia A. Vorholt − *Institute of Microbiology, ETH Zurich, 8093 Zurich, Switzerland;* orcid.org/0000-0002-6011-4910; Email: jvorholt@ethz.ch

Authors

Christoph G. Gäbelein − *Institute of Microbiology, ETH Zurich, 8093 Zurich, Switzerland*

https://doi.org/10.1021/acssynbio.2c00292
ACS Synth. Biol. 2022, 11, 3388−3396

Michael A. Reiter − *Institute of Microbiology, ETH Zurich, 8093 Zurich, Switzerland*
Chantal Ernst − *Institute of Microbiology, ETH Zurich, 8093 Zurich, Switzerland*
Gabriel H. Giger − *Institute of Microbiology, ETH Zurich, 8093 Zurich, Switzerland*

Complete contact information is available at: https://pubs.acs.org/10.1021/acssynbio.2c00292

Author Contributions

C.G.G., M.A.R., and J.A.V. designed the study. C.G.G. and C.E. performed the in vivo experiments and analyzed the data, M.A.R. designed and generated *E. coli* strains, and C.G.G. and G.H.G. produced FluidFM cantilevers. C.G.G. and J.A.V. wrote the manuscript with input from all authors.

Notes

The authors declare no competing financial interest.
All relevant data are within the paper and its Supporting Information files. The Matlab, (MatlabR2020b, MathWorks, USA) code used for image analysis is deposited online at GitLab: https://gitlab.ethz.ch/cgaebele/engineering-endosymbiotic-growth-of-e-coli/

■ ACKNOWLEDGMENTS

We thank Brett M. Barney for providing the *A. vinelandii* strain, Benjamin Daniel for providing *V. natriegens* strain, Wolf-Dietrich Hardt and Stefan Fattinger for providing the *S. enterica* strain, and Siegfried Hapfelmeier and Olivier Schaeren for providing the D-alanine *E. coli* mutant strain. We thank Tomaso Zambelli (ETH Zurich), Edin Sarajlic (SmartTip, The Netherlands), Patrick Frederix (Nanosurf AG, Switzerland), Pablo Dörig, and Dario Ossola (Cytosurge AG, Switzerland) for their support and the personnel of ETH ScopeM facility for technical assistance. We also thank Orane Guillaume-Gentil, Thomas Gassler, and Patrick R. Andreassen for helpful discussions. This work was supported by a grant from the Volkswagen foundation, Initiative "Life" (to J.A.V.), a grant from the Swiss National Science Foundation (310030B-201265) (to J.A.V.), and an European Research Council Advanced grant no. 883077 (to J.A.V.).

■ REFERENCES

(1) Martin, W.; Müller, M. The Hydrogen Hypothesis for the First Eukaryote. *Nature* **1998**, *392*, 37−41.
(2) Gould, S. B. Membranes and Evolution. *Curr. Biol.* **2018**, *28*, R381−R385.
(3) Ku, C.; Nelson-Sathi, S.; Roettger, M.; Sousa, F. L.; Lockhart, P. J.; Bryant, D.; Hazkani-Covo, E.; McInerney, J. O.; Landan, G.; Martin, W. F. Endosymbiotic origin and differential loss of eukaryotic genes. *Nature* **2015**, *524*, 427−432.
(4) Marin, B.; M. Nowack, E. C. M.; Melkonian, M. A Plastid in the Making: Evidence for a Second Primary Endosymbiosis. *Protist* **2005**, *156*, 425−432.
(5) Graf, J. S.; Schorn, S.; Kitzinger, K.; Ahmerkamp, S.; Woehle, C.; Huettel, B.; Schubert, C. J.; Kuypers, M. M. M.; Milucka, J. Anaerobic Endosymbiont Generates Energy for Ciliate Host by Denitrification. *Nature* **2021**, *591*, 445−450.
(6) Smith, T. E.; Moran, N. A. Coordination of Host and Symbiont Gene Expression Reveals a Metabolic Tug-of-War between Aphids and *Buchnera*. *Proc. Natl. Acad. Sci. U.S.A.* **2020**, *117*, 2113−2121.
(7) Markmann, K.; Parniske, M. Evolution of Root Endosymbiosis with Bacteria: How Novel Are Nodules? *Trends Plant Sci.* **2009**, *14*, 77−86.
(8) Alvarez, M.; Reynaert, N.; Chávez, M. N.; Aedo, G.; Araya, F.; Hopfner, U.; Fernández, J.; Allende, M. L.; Egaña, J. T. Generation of Viable Plant-Vertebrate Chimeras. *PLoS One* **2015**, *10*, e0130295−12.
(9) Agapakis, C. M.; Niederholtmeyer, H.; Noche, R. R.; Lieberman, T. D.; Megason, S. G.; Way, J. C.; Silver, P. A. Towards a Synthetic Chloroplast. *PLoS One* **2011**, *6*, e18877−8.
(10) Mehta, A. P.; Supekova, L.; Chen, J. H.; Pestonjamasp, K.; Webster, P.; Ko, Y.; Henderson, S. C.; McDermott, G.; Supek, F.; Schultz, P. G. Engineering Yeast Endosymbionts as a Step toward the Evolution of Mitochondria. *Proc. Natl. Acad. Sci. U.S.A.* **2018**, *115*, 11796−11801.
(11) Karas, B. J.; Moreau, N. G.; Deerinck, T. J.; Gibson, D. G.; Venter, J. C.; Smith, H. O.; Glass, J. I. Direct Transfer of a Mycoplasma Mycoides Genome to Yeast Is Enhanced by Removal of the Mycoides Glycerol Uptake Factor Gene GlpF. *ACS Synth. Biol.* **2019**, *8*, 239−244.
(12) Sulo, P.; Griač, P.; Klobučníková, V.; Kováč, L. A Method for the Efficient Transfer of Isolated Mitochondria into Yeast Protoplasts. *Curr. Genet.* **1989**, *15*, 1−6.
(13) Goetz, M.; Bubert, A.; Wang, G.; Chico-Calero, I.; Vazquez-Boland, J. A.; Beck, M.; Slaghuis, J.; Szalay, A. A.; Goebel, W. Microinjection and Growth of Bacteria in the Cytosol of Mammalian Host Cells. *Proc. Natl. Acad. Sci. U.S.A.* **2001**, *98*, 12221−12226.
(14) Wu, T.; Teslaa, T.; Kalim, S.; French, C. T.; Moghadam, S.; Wall, R.; Miller, F.; Witte, X. O. N.; Teitell, M. A.; Chiou, P. Photothermal Nanoblade for Large Cargo Delivery into Mammalian Cells. *Anal. Chem.* **2011**, *83*, 1321−1327.
(15) Meister, A.; Gabi, M.; Behr, P.; Studer, P.; Vörös, J.; Niedermann, P.; Bitterli, J.; Polesel-Maris, J.; Liley, M.; Heinzelmann, H.; Zambelli, T. FluidFM: Combining Atomic Force Microscopy and Nanofluidics in a Universal Liquid Delivery System for Single Cell Applications and Beyond. *Nano Lett.* **2009**, *9*, 2501−2507.
(16) Guillaume-Gentil, O.; Potthoff, E.; Ossola, D.; Franz, C. M.; Zambelli, T.; Vorholt, J. A. Force-Controlled Manipulation of Single Cells: From AFM to FluidFM. *Trends Biotechnol.* **2014**, *32*, 381−388.
(17) Guillaume-Gentil, O.; Potthoff, E.; Ossola, D.; Dörig, P.; Zambelli, T.; Vorholt, J. A. Force-Controlled Fluidic Injection into Single Cell Nuclei. *Small* **2013**, *9*, 1904−1907.
(18) Giannella, R. A.; Washington, O.; Gemski, P.; Formal, S. B. Invasion of HeLa Cells By *Salmonella typhimurium*: A Model for Study of Invasiveness of *Salmonella*. *J. Infect. Dis.* **1973**, *128*, 69−75.
(19) Gäbelein, C. G.; Feng, Q.; Sarajlic, E.; Zambelli, T.; Guillaume-Gentil, O.; Kornmann, B.; Vorholt, J. A. Mitochondria Transplantation between Living Cells. *PLoS Biol.* **2022**, *20*, No. e3001576.
(20) Vaudaux, P.; Waldvogel, F. A. Gentamicin Antibacterial Activity in the Presence of Human Polymorphonuclear Leukocytes. *Antimicrob. Agents Chemother.* **1979**, *16*, 743−749.
(21) Akagi, J.; Kordon, M.; Zhao, H.; Matuszek, A.; Dobrucki, J.; Errington, R.; Smith, P. J.; Takeda, K.; Darzynkiewicz, Z.; Wlodkowic, D. Real-Time Cell Viability Assays Using a New Anthracycline Derivative DRAQ7. *Cytometry, Part A* **2013**, *83A*, 227−234.
(22) Amarante-Mendes, G. P.; Adjemian, S.; Branco, L. M.; Zanetti, L. C.; Weinlich, R.; Bortoluci, K. R. Pattern Recognition Receptors and the Host Cell Death Molecular Machinery. *Front. Immunol.* **2018**, *9*, 1−19.
(23) Kentner, D.; Martano, G.; Callon, M.; Chiquet, P.; Brodmann, M.; Burton, O.; Wahlander, A.; Nanni, P.; Delmotte, N.; Grossmann, J.; Limenitakis, J.; Schlapbach, R.; Kiefer, P.; Vorholt, J. A.; Hiller, S.; Bumann, D. Shigella Reroutes Host Cell Central Metabolism to Obtain High-Flux Nutrient Supply for Vigorous Intracellular Growth. *Proc. Natl. Acad. Sci. U.S.A.* **2014**, *111*, 9929−9934.
(24) Røst, L. M.; Brekke Thorfinnsdottir, L. B.; Kumar, K.; Fuchino, K.; Eide Langørgen, I. E.; Bartosova, Z.; Kristiansen, K. A.; Bruheim, P. Absolute Quantification of the Central Carbon Metabolome in Eight Commonly Applied Prokaryotic and Eukaryotic Model Systems. *Metabolites* **2020**, *10*, 74.
(25) Yang, J. I.; Hwang, J. S.; Camakaris, H.; Irawaty, W.; Ishihama, A.; Pittard, J. Mode of action of the TyrR protein: repression and

activation of the tyrP promoter of Escherichia coli. *Mol. Microbiol.* **2004**, *52*, 243−256.
(26) Sarsero, J. P.; Wookey, P. J.; Gollnick, P.; Yanofsky, C.; Pittard, A. J. A New Family of Integral Membrane Proteins Involved in Transport of Aromatic Amino Acids in *Escherichia coli*. *J. Bacteriol.* **1991**, *173*, 3231−3234.
(27) Brown, K. D. Formation of Aromatic Amino Acid Pools in *Escherichia coli* K-12. *J. Bacteriol.* **1970**, *104*, 177−188.
(28) Pi, J.; Wookey, P. J.; Pittard, A. J. Cloning and Sequencing of the PheP Gene, Which Encodes the Phenylalanine-Specific Transport System of *Escherichia coli*. *J. Bacteriol.* **1991**, *173*, 3622−3629.
(29) Hiraga, S.; Ito, K.; Matsuyama, T.; Ozaki, H.; Yura, T. 5-Methyltryptophan-Resistant Mutations Lniked with the Arginine G Marker in *Escherichia coli*. *J. Bacteriol.* **1968**, *96*, 1880−1881.
(30) Ames, G. F. L.; Nikaido, K. Identification of a Membrane Protein as a Histidine Transport Component in Salmonella Typhimurium. *Proc. Natl. Acad. Sci. U.S.A.* **1978**, *75*, 5447−5451.
(31) Liao, M. K.; Gort, S.; Maloy, S. A Cryptic Proline Permease in Salmonella Typhimurium. *Microbiology* **1997**, *143*, 2903−2911.
(32) Nazos, P. M.; Mayo, M. M.; Su, T. Z.; Anderson, J. J.; Oxender, D. L. Identification of LivG, a Membrane-Associated Component of the Branched-Chain Amino Acid Transport in *Escherichia coli*. *J. Bacteriol.* **1985**, *163*, 1196−1202.
(33) Nazos, P. M.; Antonucci, T. K.; Landick, R.; Oxender, D. L. Cloning and Characterization of LivH, the Structural Gene Encoding a Component of the Leucine Transport System in *Escherichia coli*. *J. Bacteriol.* **1986**, *166*, 565−573.
(34) Frankel, G.; Ron, E. Z. Escherichia coli, a Versatile Pathogen. *Current Topics in Microbiology and Immunology*; Springer, 2018; Vol. *340*.
(35) Ray, K.; Marteyn, B.; Sansonetti, P. J.; Tang, C. M. Life on the inside: The Intracellular Lifestyle of Cytosolic Bacteria. *Nat. Rev. Microbiol.* **2009**, *7*, 333−340.
(36) Sauer, J. D.; Herskovits, A. A.; O'Riordan, M. X. D. Metabolism of the Gram-Positive Bacterial PathogenListeria monocytogenes. *Gram-Positive Pathog.* **2019**, *11262*, 864−872.
(37) Guillaume-Gentil, O.; Gäbelein, C. G.; Schmieder, S.; Martinez, V.; Zambelli, T.; Künzler, M.; Vorholt, J. A. Injection into and Extraction from Single Fungal Cells. *Commun. Biol.* **2022**, *5*, 180.
(38) Cuenca, M.; Pfister, S. P.; Buschor, S.; Bayramova, F.; Hernandez, S. B.; Cava, F.; Kuru, E.; Van Nieuwenhze, M. S.; Brun, Y. V.; Coelho, F. M.; Hapfelmeier, S. D-Alanine-Controlled Transient Intestinal Mono-Colonization with Non-Laboratory-Adapted Commensal *E. coli* Strain HS. *PLoS One* **2016**, *11*, e0151872−17.
(39) Moran, N. A.; Wernegreen, J. J. Lifestyle evolution in symbiotic bacteria: insights from genomics. *Trends Ecol. Evol.* **2000**, *15*, 321−326.
(40) Muller, H. J. The Relation of Recombination to Mutational Advance. *Mutat. Res., Fundam. Mol. Mech. Mutagen.* **1964**, *1*, 2−9.
(41) Douglas, A. E. How Multi-Partner Endosymbioses Function. *Nat. Rev. Microbiol.* **2016**, *14*, 731−743.
(42) Dos Santos, P. *Molecular Biology and Genetic Engineering in Nitrogen Fixation*; Springer Science+Business Media, 2011.
(43) Schindelin, J.; Arganda-Carreras, I.; Frise, E.; Kaynig, V.; Longair, M.; Pietzsch, T.; Preibisch, S.; Rueden, C.; Saalfeld, S.; Schmid, B.; Tinevez, J.-Y.; White, D. J.; Hartenstein, V.; Eliceiri, K.; Tomancak, P.; Cardona, A. Fiji: An Open-Source Platform for Biological-Image Analysis. *Nat. Methods* **2012**, *9*, 676−682.
(44) Thyng, K. M.; Greene, C. A.; Hetland, R. D.; Zimmerle, H. M.; DiMarco, S. F. True Colors of Oceanography: Guidelines for Effective and Accurate Colormap Selection. *Oceanography* **2016**, *29*, 9−13.
(45) Jiang, Y.; Chen, B.; Duan, C.; Sun, B.; Yang, J.; Yang, S. Multigene Editing in the Escherichia Coli Genome via the CRISPR-Cas9 System. *Appl. Environ. Microbiol.* **2015**, *81*, 2506−2514.
(46) Guo, J.; Wang, T.; Guan, C.; Liu, B.; Luo, C.; Xie, Z.; Zhang, C.; Xing, X. H. Improved SgRNA Design in Bacteria via Genome-Wide Activity Profiling. *Nucleic Acids Res.* **2018**, *46*, 7052−7069.
(47) Wang, H. H.; Church, G. M. *Multiplexed Genome Engineering and Genotyping Methods: Applications for Synthetic Biology and Metabolic Engineering*, 1st ed.; Elsevier Inc., 2011; Vol. *498*.

https://doi.org/10.1021/acssynbio.2c00292
ACS Synth. Biol. 2022, 11, 3388−3396